

Boundary Element Analysis of Multiple Seismic Crack Propagation in Concrete Gravity Dams

V. Batta¹ and O.A. Pekau²

ABSTRACT

The previously developed two-dimensional boundary element procedure for analyzing the propagation of a single discrete crack is extended to simultaneous multiple cracking in concrete gravity dams. Both single and multiple cracking models are employed to investigate the fracture response of the Koyna dam. The final rupture in the dam as well as the fracture process itself are examined in particular. Similar final damage involving complete separation of the crest block of the dam is predicted, irrespective of whether single or multiple crack propagation models are employed.

INTRODUCTION

Linear seismic response analyses (Chopra and Chakrabarti, 1973), experimental investigations (Niwa and Clough, 1980) and past experiences (Ahmadi and Khoshrang, 1992) all have demonstrated that concrete gravity dams develop tensile cracks when subjected to strong enough ground shaking from an earthquake. Non-linear dynamic fracture analysis procedures are therefore required to assess the extent and significance of potential cracking in existing dams as well as in those under design. Although the finite element method is equally adaptable (Ayari and Saouma, 1990; Bhattacharjee and Léger, 1993), the boundary element technique has certain unique features which recommend it for such analyses. Primarily, the method requires discretization only of the boundary of the structure and utilizes the exact solution of the governing equations in the interior, thus leading to enhanced accuracy. Discrete crack modelling and crack propagation criteria based on fracture mechanics can also be easily incorporated, as demonstrated recently by Pekau and Batta (1994) and Pekau et al. (1995). Although the latter were the first attempts at employing the boundary element method for the dam fracture problem, the procedures accounted for only a single crack in the dam.

In the present work, the previous formulation by the authors is extended to the more general case where the occurrence and simultaneous propagation of multiple cracks can be simulated. A detailed examination of the cracking process for the Koyna dam employing both single and multiple fracture models is presented with particular attention focussed on the patterns of rupture predicted by these fracture models.

MODELLING AND MONITORING OF MULTIPLE CRACKS

In modelling a dam body containing discrete cracks, the boundary element technique requires that the crack surfaces, which obviously have identical spatial location, belong to two different dam domains. This is achieved by dividing the dam into sub-domains utilizing an arbitrary line which extends from the

^I Research assistant, Concordia University; also Structural Engineer, SNC-Lavalin Inc., Montreal.

^{II} Professor, Dept. of Civil Engineering, Concordia University, Montreal, Que. H3G 1M8.

crack tip to the opposite boundary. The crack flank nodes belong to the adjacent sub-domains, whereas the common nodes along the interface ahead of the crack tip provide continuity of displacement and equilibrium of tractions between the two sub-domains. The boundary of the system, as well as the interfaces between sub-domains, is discretized and the global matrix equation is assembled. Details of this procedure along with the analytical formulation are available in Pekau and Batta (1992).

When more cracks than one are present, the domain surrounding each crack is divided into sub-regions. If any two cracks exist at nearly the same elevation but on opposite faces of the dam, the same arbitrary line could be employed as the dividing line, but in the present computer implementation separate lines are used. This provides better control during discretization following crack propagation, although each additional crack increases the number of sub-domains by one.

The analytical modelling of stress singularity at discrete crack tips is achieved by providing traction singular quarter-point elements consistent with the concepts of linear elastic fracture mechanics. To simulate the induced mixed mode of cracking, both mode I and II stress intensity factors are computed employing the displacement correlation technique. Maximum tensile strain theory is employed to monitor crack stability, based on the dynamic fracture toughness K_{I_d} of concrete. When a crack is detected to be unstable, the direction of crack propagation is computed and the boundary element mesh along the crack line is appropriately modified by moving forward the crack tip and relocating the interface nodes. If during the analysis multiple cracks lie close to each other, it is possible that one of the crack tips advances towards the interface line corresponding to an adjacent crack. In such a case, the affected sub-domain boundary needs to be relocated to accommodate the extending crack. The problem can, however, be more easily circumvented by judiciously choosing the initial orientations of the interface boundaries so that they are less likely to interfere with crack development.

SINGLE AND MULTIPLE CRACKING OF KOYNA DAM

Koyna dam is a 103 m high concrete gravity dam in India which was constructed in 1963 and subjected to magnitude 6.5 earthquake on December 11, 1967. Significant horizontal cracking was noticed in a number of the non-overflow monoliths on the upstream, the downstream or on both faces. Leakage was observed in some of these monoliths from approximately horizontal cracks near the elevation of slope change on the downstream face, thus implying complete penetration from one face to the other.

The cross-section of the tallest non-overflow monolith of the dam is shown in Fig. 1(a). This dam has a non-typical cross-section resulting from a change made during construction when it was decided to build the dam to its full height in one stage rather than the planned two stages. In the analysis, the following material characteristics are used for the concrete: modulus of elasticity $E = 31$ GPa; Poisson's ratio $\nu = 0.2$; and mass density $\gamma = 2640$ kg/m³. The concrete compressive and tensile strengths are assumed to be 30 MPa and 3 MPa, respectively. In the absence of any test data for the Koyna concrete, the dynamic fracture toughness K_{I_d} is assumed to be 2.0 MPa.m^{1/2}. However, due to the uncertainty concerning the magnitude of this parameter, the influence of increasing K_{I_d} to 5.5 and 9.0 MP.m^{1/2} is investigated also. The dam is considered fixed at the base and the hydrodynamic effect of the reservoir (headwater elevation 92.0 m) is modelled approximately by Westergaard added mass. Damping equal to 5 per cent is assumed for the first two modes of vibration. Water pressure effects in the cracks are not included in the analysis, since no model for hydrodynamic interaction in cracks propagating under seismic action exists to the authors' knowledge.

Potential cracking models

In order to predict the locations of potential cracking, stress analysis of the intact dam subjected to 6

sec of vertical and horizontal accelerations of the recorded Koyna earthquake is first performed. Envelope values of the resulting principal tensile stresses are presented in Fig. 1(b), where it is seen that the tensile stresses exceed the tensile strength of concrete near elevation 66.5 m on both the downstream and the upstream faces (zones 1 and 2, respectively). On the downstream face, due to the change in slope at this elevation, the stress singularity results in a computed maximum tensile stress almost three times the tensile strength of concrete. Another zone of high tensile stress is obtained on the upstream face near the base (zone 3). However, since the observed cracking in the Koyna dam is limited to zones 1 and 2 only, in the present study cracking of the dam is investigated in these regions. Fracture in zone 3 was also considered but an initial crack modelled at this location did not propagate during seismic analysis.

Based on the above, three different sets of small cracks are pre-assigned on the faces of the dam and the fracture response of the dam is investigated for each of these three models of cracking. In the first two, a single 1 m long initial crack is introduced separately on the downstream and the upstream faces of the dam, cracks C1 and C2 at elevations 66.5 and 70.0 m respectively, whereas in the third case a multiple cracking model is assumed with cracks C1 and C2 originating simultaneously on both faces of the dam. The corresponding boundary element discretizations for these cracking models are depicted in Fig. 2.

Envelopes of the principal tensile stresses on the faces of the dam are presented in Fig. 3 for the three cracking models. For the models with a single crack, Figs. 3(a) and 3(b) show that the tensile stresses on both faces of the dam are reduced to levels below the strength of concrete. Thus it appears that, if the initial cracking originates on either face, other cracking will not develop before the initial crack has broken through to the opposite face. Similar behavior is observed in Fig. 3(c) for cracks C1 and C2 propagating from both faces. Unlike the preceding two fracture models, however, this analysis was able to be continued for a substantially longer period of time prior to rupture, allowing the dam to be subjected to the more intense portion of the Koyna earthquake. In spite of this increase in ground shaking, the stress release caused by cracking is seen still to reduce the maximum tensile stress to below the strength of the concrete. Simultaneous other cracking is therefore not predicted to occur in the dam for this fracture model also.

It is therefore evident that the model for the actual cracking of the dam is most likely to be associated only with zone 1. However, because initial cracks are not solely stress-induced but may also arise due to a variety of other causes including shrinkage, temperature effects, etc., the additional two fracture models are included in the following examination of the fracture process of the Koyna dam. Moreover, for dams of other geometries involving more typical cross-sections, all the above three cracking models become possible candidates for the critical fracture process.

Comparison of fracture processes for single and multiple cracking models

Results for seismic crack propagation for the three fracture models are depicted in Figs. 4 and 5. As shown in Fig. 4, the final cracking profiles for the single fracture models are more or less similar, with the initial crack breaking through to the opposite face of the dam to cause complete rupture. Analogous final behavior is predicted by the multiple fracture analysis, in which cracks C1 and C2 merge within the body of the dam and also result in full separation of the crest block; however, the final rupture pattern for this model differs markedly from the profiles of the single fracture models. Instantaneous geometry of a crack is seen to influence the propagation path followed by the crack on the opposite face of the dam. Thus, comparing Figs. 4(a) and 4(c), the influence of C2 on crack C1 is only evident toward the end of the propagation of the latter because, as discussed below, crack C1 completes its propagation while upstream crack C2 is still short. On the other hand, the final trajectories of crack C2 are noticeably different in Figs. 4(b) and 4(c). With crack C1 already developed in Fig. 4(c) for the multiple cracking model, a change in

the orientation of the stress field in front of the crack tip causes C2 to bend downwards. This change in stress field orientation is due to the increase in shear stress which occurs in the intact concrete ahead of the crack tip when the crest deflects in the downstream direction.

Time histories of crack propagation for the three fracture models are shown in Fig. 5. Time history data for the single cracking models indicate that these cracks propagate almost instantaneously to penetrate through the entire width of the dam. Instability of crack C1 of Fig. 5(a) is first detected at 2.46 sec and the crack propagation is completed in the next few time steps, with a total elapsed time of 0.03 sec. The single upstream crack C2 of Fig. 5(b) begins to propagate even earlier, at 2.27 sec, and penetrates the dam in 0.015 sec without arresting. Unlike this abrupt fracture behavior, the propagation of cracks C1 and C2 of multiple cracking model each comprises two distinct phases as shown in Fig. 5(c). It is seen that the downstream crack C1 is the first to grow, becoming unstable at 2.46 sec and propagating in two stages. In the first, this crack extends rapidly by about 15 m in 0.03 sec. As the crest movement reverses, the crack temporarily stabilizes but begins again to propagate when the dam crest deflects toward the upstream in the next cycle. This second stage of growth comprises a crack extension of about 4 m in 0.01 sec. At 3.8 sec, upstream crack C2 extends also in two phases. In this process, the tip of C2 approaches sufficiently close to crack C1 so that further propagation analysis would cause the sub-domain boundaries emanating from the two crack tips to intersect. It is therefore assumed that the upstream crack merges into the downstream crack at this time, resulting in complete rupture along the dashed line in Fig. 4(c).

Behavior with higher concrete fracture toughness

Since multiple cracking has been predicted previously (Pekau and Batta, 1994) for higher magnitude of concrete fracture toughness, the analysis is performed only for the multiple fracture model. The final crack trajectories for $K_{I_d} = 5.5$ and $9.0 \text{ MPa}\cdot\text{m}^{1/2}$ are presented in Fig. 6. It is evident that substantially different cracking patterns are obtained for these two toughness values. For $K_{I_d} = 5.5 \text{ MPa}\cdot\text{m}^{1/2}$ the two cracks propagate into the dam and merge with each other, resulting in a final rupture pattern very similar to that for $K_{I_d} = 2.0 \text{ MPa}\cdot\text{m}^{1/2}$. The details of the associated crack propagation processes (not discussed herein), however, differ considerably.

In the absence of any significant upstream cracking for $K_{I_d} = 9.0 \text{ MPa}\cdot\text{m}^{1/2}$, the principal tensile stress envelope for this case is examined in Fig. 7. The delayed propagation of the downstream crack, due to the high fracture toughness combined with the short final length of the upstream crack, results in keeping the tensile stresses high throughout the dam faces. Thus, it appears that higher magnitude of concrete fracture toughness indeed results in distributing the surface cracking in the dam as predicted previously, but these cracks do not necessarily propagate if the concrete toughness is sufficiently high.

CONCLUSIONS

The performance of the boundary element procedure for the analysis of multiple cracking in concrete gravity dams is demonstrated in this work. For the Koyna dam, the critical cracking is found to be associated with fracture originating at the point of downstream slope change and penetrating the dam almost instantaneously. Although the multiple fracture model also indicates complete rupture, the corresponding fracture process itself is considerably different when compared with those for single fracture. Increasing the concrete fracture toughness from 2.0 to $5.5 \text{ MPa}\cdot\text{m}^{1/2}$ does not appear to affect the predicted final cracking in the dam. Furthermore, for higher magnitudes of toughness cracking in the dam becomes distributed but with most of the cracks confined to the surface.

ACKNOWLEDGEMENTS

This research was supported by Grant No. A8258 from the Natural Sciences and Engineering Research Council of Canada. The advice of Professor Zhang Chuhan of Tsinghua University, Beijing, during various stages of this work is also gratefully acknowledged.

REFERENCES

- Ahmadi, M. T. and Khoshrang, Gh. 1992. 'Sefidrud dam's dynamic response to large near-field earthquake of June 1990', *Dam Engineering*, 5(2), 85-115.
- Ayari, M. L. and Saouma, V.E. 1993. 'A fracture mechanics based seismic analysis of concrete gravity dams using discrete cracks', *Engineering Fracture Mechanics*, 35(1/2/3), 587-598.
- Bhattacharjee, S. S. and Léger, P. 1993. 'Seismic cracking and energy dissipation in concrete gravity dams', *Earthquake Engineering and Structural Dynamics*, 22, 991-1007.
- Chopra, A. K. and Chakrabarti, P. 1973. 'The Koyna earthquake and damage to Koyna dam', *Bulletin of the Seismological Society of America*, 63, 381-397.
- Niwa, A. and Clough, R. W. 1980. 'Shaking table research on concrete dam models', Report No. UCB/EERC 80/05, Earthquake Engineering Research Center, University of California, Berkeley.
- Pekau, O. A. and Batta, V. 1994. 'Seismic cracking behavior of concrete gravity dams', *Dam Engineering*, 5(1), 5-29.
- Pekau, O. A., Lingmin, F. and Chuhan, Z. 1995. 'Seismic cracking of Koyna dam: Case study', *Earthquake Engineering and Structural Dynamics*, 24, 15-33.
- Pekau, O. A. and Batta, V. 1992. 'Seismic crack propagation analysis of concrete structures using boundary elements', *International Journal for Numerical Methods in Engineering*, 35, 1547-1564.

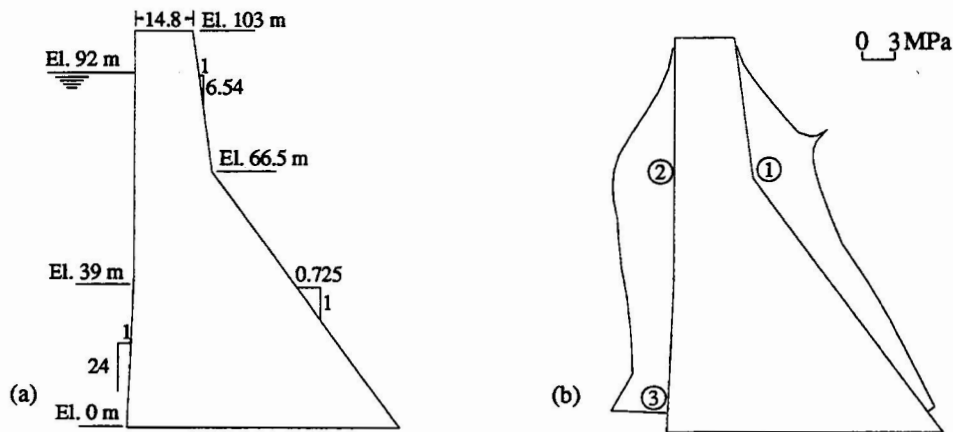


Figure 1. Koyna dam: (a) tallest non-overflow monolith; (b) envelope of principal tensile stresses for seismic analysis without cracks

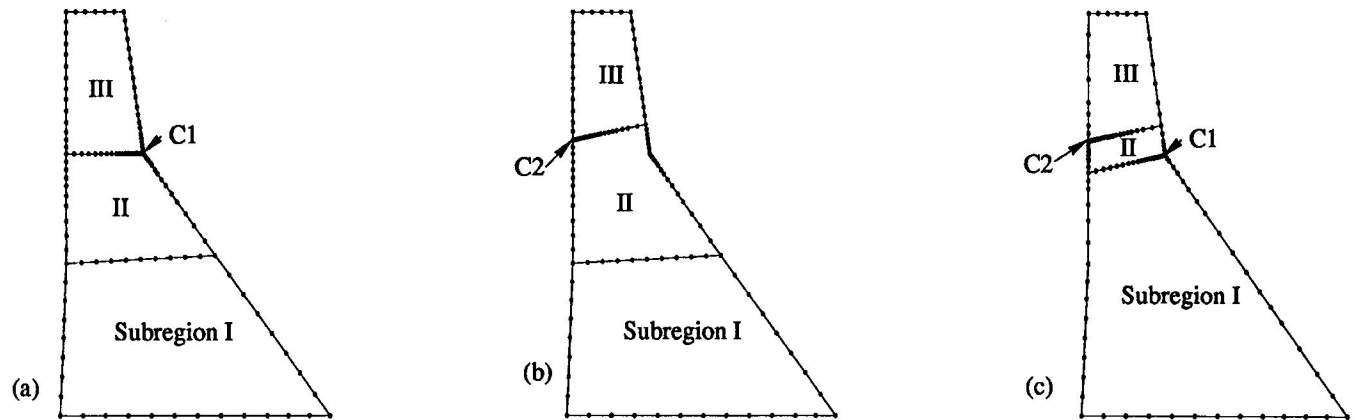


Figure 2. Boundary element discretizations of Koyna dam for different fracture models: (a) single downstream crack C1; (b) single upstream crack C2; (c) multiple cracking

362

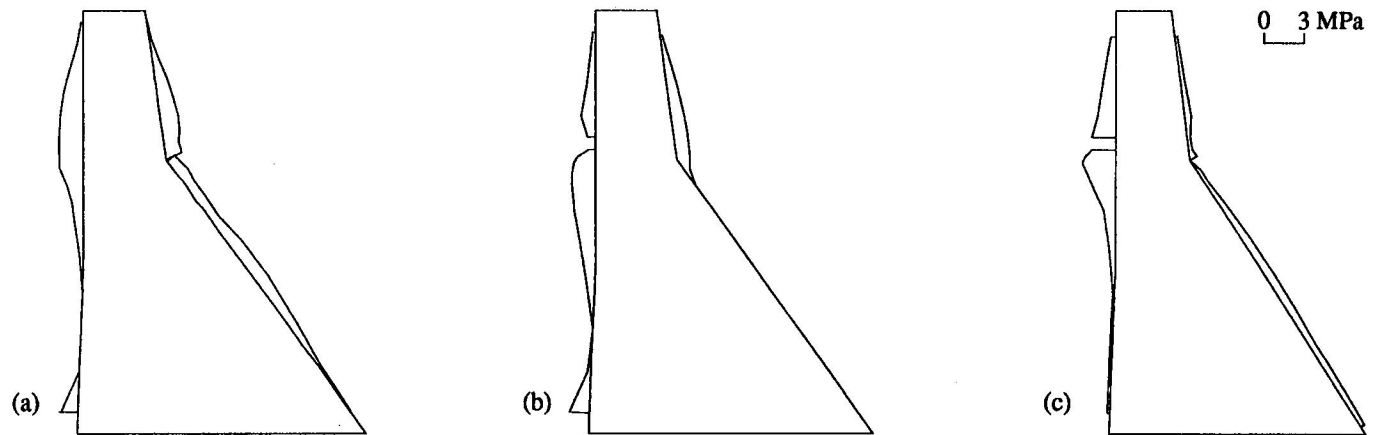


Figure 3. Envelopes of principal tensile stresses for different fracture models: (a) single downstream crack C1; (b) single upstream crack C2; (c) multiple cracking

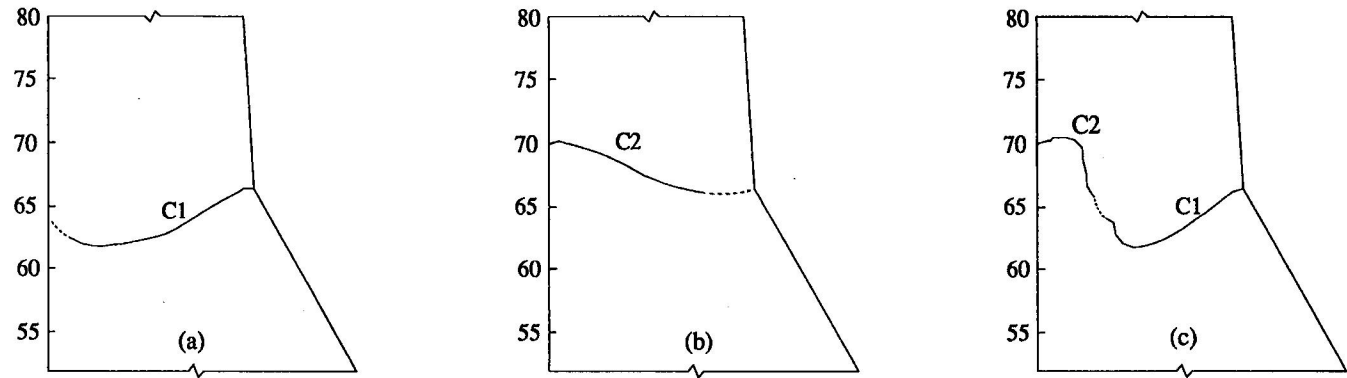


Figure 4. Final fracture patterns: (a) single downstream crack C1; (b) single upstream crack C2; (c) multiple cracks C1 and C2

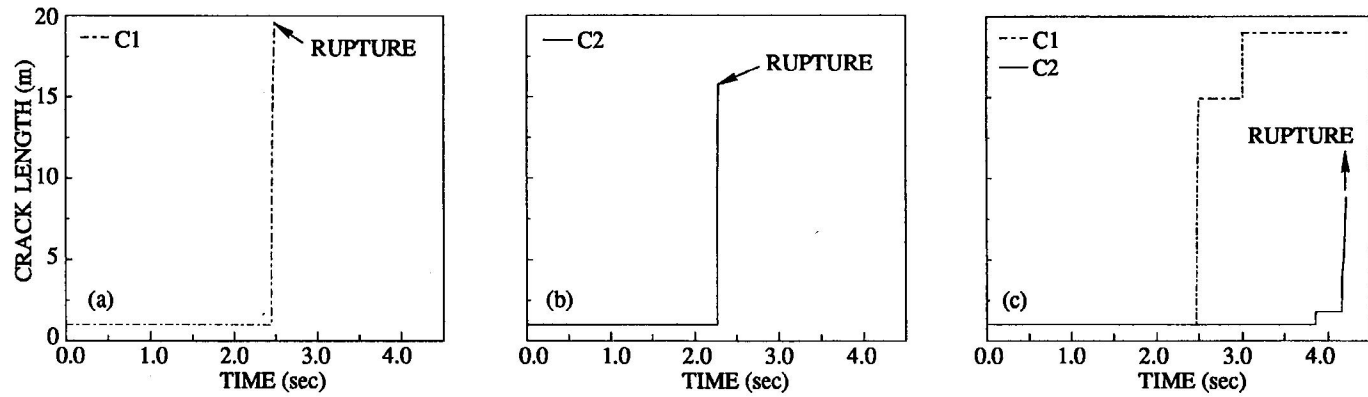


Figure 5. Time histories of crack propagation: (a) single downstream crack C1; (b) single upstream crack C2; (c) multiple cracks C1 and C2

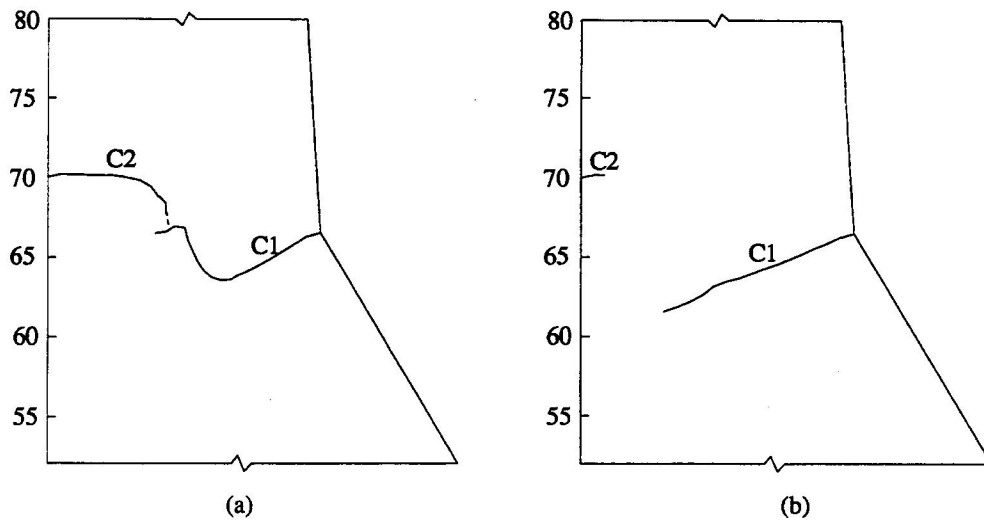


Figure 6. Final cracking profiles for multiple fracture model and higher magnitudes of dynamic fracture toughness: $K_{Id} = 5.5 \text{ MPa.m}^{1/2}$; (b) $K_{Id} = 9.0 \text{ MPa.m}^{1/2}$

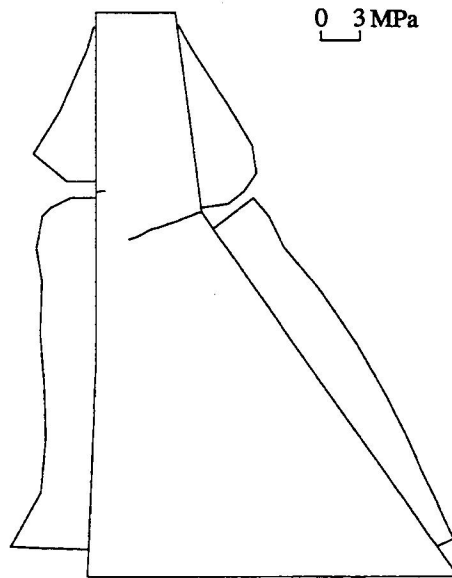


Figure 7. Envelope of principal tensile stresses for multiple cracking model and $K_{Id} = 9.0 \text{ MPa.m}^{1/2}$